Copy
RM L57H15

NACA RM L57H15

NACA

RESEARCH MEMORANDUM

A HYDROGEN PEROXIDE TURBOJET-ENGINE SIMULATOR FOR WIND-TUNNEL POWERED-MODEL INVESTIGATIONS

By Jack F. Runckel and John M. Swihart

Langley Aeronautical Laboratory
Langley Field, Va.

NATIONAL ADVISORY COMMITTEE
FOR AERONAUTICS

WASHINGTON
November 4, 1957
Declassified January 12, 1961

NACA RM L57H15

NATIONAL ADVISORY COMMITTEE FOR AERONAUTICS

RESEARCH MEMORANDUM

A HYDROGEN PEROXIDE TURBOJET-ENGINE SIMULATOR FOR WIND-TUNNEL POWERED-MODEL INVESTIGATIONS

By Jack F. Runckel and John M. Swihart

SUMMARY

A turbojet-engine-exhaust simulator which utilizes a hydrogen peroxide gas generator has been developed for powered-model testing in wind tunnels with air exchange. Catalytic decomposition of concentrated hydrogen peroxide is shown to provide a convenient and easily controlled method of providing a hot jet whose characteristics correspond closely to the jet of a gas-turbine engine.

The problems associated with jet exhaust simulation in a transonic wind tunnel which led to the selection of a liquid monopropellant are discussed. The operation of the jet simulator consisting of a thrust balance, gas generator and exit nozzle, and auxiliary control system is described. Static-test data obtained with convergent nozzles are presented and shown to be in good agreement with ideal calculated values.

INTRODUCTION

It has long been recognized that jet effects are responsible for a number of the differences between drag, stability, and loads results obtained in flight tests and in the usual wind-tunnel investigations. Because of importance of these effects, methods for simulating jets were developed for subsonic and supersonic tunnels (refs. 1 and 2) and for rocket models (ref. 3). The problem of simulation at transonic speeds, however, was found to be much more difficult because of the much greater importance of support interference effects. One early transonic-jet program (ref. 4) utilized a simulation scheme similar to that for references 1 and 2 and relied on point by point analysis of schlieren photographs and pressure distributions to determine the onset and magnitude of support interference effects. In a second scheme for transonic simulation (refs. 5 and 6), support interference is eliminated by using an apparatus consisting of a cylindrical tube extending downstream from the

settling chamber to the test section of a small transonic-tunnel nozzle. This latter scheme generally requires small model size and necessitates a careful evaluation of the effects of an unduly thick initial boundary layer.

A simulation scheme was desired which would permit detailed study of installation problems and jet interference effects using complete or essentially complete models. The primary characteristics desired were large model size, minimum support interference, and sufficiently close duplication of turbojet exhaust characteristics to permit valid studies of the interactions of such a jet with both internal and external flows.

After considering several methods of producing a hot jet which would simulate the characteristics of turbojet-engine exhausts and a system that would require a minimum of space inside the model and support, the liquid monopropellant hydrogen peroxide was selected. The literature revealed that hydrogen peroxide had been used as a successful gas generator for turbopump turbine drives (refs. 7 and 8). Considerable experience with the liquid as a propellant was available (ref. 9), so it was expected that little development work would be required to adapt this system for research.

It is the purpose of this paper to describe a hydrogen peroxide jet simulator which can be used for powered-model testing in wind tunnels with air exchange and to indicate the necessary associated equipment. This simulator system was developed to meet the specific needs of the Langley 16-foot transonic tunnel. Some information pertaining to this system has been reported in reference 10. The results of static tests on some engine turbojet tailpipe configurations using the hydrogen peroxide technique are discussed in the present paper.

SYMBOLS

A	jet-exit area, sq ft
C_F	thrust coefficient, F_j/qS
$C_{F,O}$	static thrust coefficient, F_j/Ap_O
C_d	discharge coefficient, w/w_i
$\frac{F_j}{F_i}$	thrust ratio
d	diameter

F_j measured jet thrust

F_i ideal thrust for complete isentropic expansion of primary flow,

$$w\sqrt{\frac{2R}{g}\frac{\gamma}{\gamma - 1}T_{t,j}\left[1 - \left(\frac{p_0}{p_{t,j}}\right)^{\frac{\gamma-1}{\gamma}}\right]}$$

$F_{i,c}$ ideal convergent nozzle thrust, for choked flow,

$$\frac{w}{g}\sqrt{\gamma g R \frac{2}{\gamma + 1}T_{t,j}} + A\left(p_j - p_0\right)$$

g acceleration due to gravity, ft/sec^2

p static pressure, lb/ft^2

p_t total pressure, lb/ft^2

q dynamic pressure, lb/ft^2

R gas constant, $ft/^oR$

r average radius of curvature of jet boundary

S wing area, sq ft

T temperature, ^oR

t temperature, ^oF

V velocity, ft/sec

w weight flow, lb/sec

w_i ideal weight flow for choked exit,

$$p_{t,j}A_j\left(\frac{2}{\gamma + 1}\right)^{\frac{\gamma+1}{2(\gamma-1)}}\sqrt{\frac{\gamma g}{RT_{t,j}}}$$

w_∞ equivalent stream flow through jet exit, $gA\rho_\infty V_\infty$, lb/sec

$\frac{w_s}{w_p}\sqrt{\frac{T_{t,s}}{T_{t,p}}}$ corrected secondary-to-primary weight-flow ratio

x distance from decomposition-chamber inlet

γ ratio of specific heats

δ angle between jet axis and tangent to free jet boundary at nozzle lip, deg

ρ mass density, slugs/ft^3

Subscripts:

j jet

p primary

s secondary

t total

0 ambient

∞ free stream

FLOW-SIMILARITY CONSIDERATIONS

A propulsive jet affects the airplane through both direct reactions and interferences. In certain free-flight and stability and performance investigations (refs. 3 and 11), complete simulation of both items may be required. For the majority of wind-tunnel investigations, however, it is only necessary to duplicate the interference effects. Primary attention was focused on this latter more restricted problem in the development of a jet simulation system considered herein. Simulation of the jet intake flow may not be necessary if the external-flow field in the vicinity of the exit is similar to that of the airplane. Numerous drag investigations have provided a broad background of information concerning the interference effects of intake flow in the transonic-speed range.

In discussing interference effects due to a propulsive jet, it is convenient to break the jet flow down into two regions: the jet bulb immediately downstream of the exit and the trailing mixing region. With a given set of external-flow conditions, the initial shape of the jet boundary is determined mainly by the ratio of specific heats and nozzle-exit pressure ratio of the jet flow (ref. 12). A number of investigations (e.g., refs. 6, 13, and 14) have indicated that duplication of the slope of this segment of the jet boundary is all that is required in studies

of the base and boattail drag of afterbodies without appreciable flow separation and external interference effects associated with the initial (exit) shock. This finding is of great practical significance with regard to simulator selection, inasmuch as a jet with an incorrect ratio of specific heats can be used to simulate the boundary of a real jet because the correct initial boundary shape still can be obtained by operating the simulator at some arbitrary exit pressure ratio.

As pointed out in reference 10, the characteristics of the jet downstream of the initial expansion are determined by a number of internal jet flow properties in addition to the specific heat ratio and the nozzle-exit pressure ratio. For example, when the external stream is supersonic, the internal jet shock penetrates the mixing boundary into the free stream and forms a second external shock system downstream of the exit shock. When the external flow is subsonic, the internal shock, instead of penetrating into the external flow, reflects from the interface and forms the familiar shock diamonds which result in a somewhat wavy jet boundary. (See ref. 15.) In either case, simulation of the downstream shock structure obviously involves duplication of the exit Mach number and nozzle shape, as well as exact duplication of the exit-pressure ratio and ratio of specific heats. This degree of simulation would appear to be adequate for most studies of downstream shock interference effects.

Complete representation of the interference effects of the downstream jet requires duplication of the mixing processes along the jet boundary, in addition to all the items mentioned previously. These mixing processes are governed by the viscosities, momentums, and heat transfer rates of the local elements of mixing flow so that complete simulation involves essential duplication of the actual jet engine exhaust. This degree of duplication obviously is not needed in most flow-field studies. It may be justified, however, in investigations wherein flow entrainment along the jet boundary and jet-area displacement effects play a major role. For example, changes in jet temperature have been found to have effects of major significance in investigations of: (1) afterbodies with appreciable flow separation (refs. 2, 4, and 13), (2) exit configurations with secondary cooling or ejector flows (ref. 16), and (3) afterburner arrangements (ref. 17). In such cases, departures from complete simulation can only be justified on the basis of experience.

After study of the flow-similarity considerations just discussed, it was decided that the jet simulation system of the Langley 16-foot transonic tunnel must provide a hot jet with gas properties sufficiently close to those for turbojet exhausts to permit reasonably accurate duplication of mixing phenomena and downstream flow-field effects, as well as the more easily simulated flow conditions in the immediate vicinity of the nozzle exit. Inasmuch as the preliminary jet-effects work in the Langley 8-foot transonic tunnel (ref. 4) had considerably clarified the

nature of the jet simulation problem, attention was focused on obtaining close jet simulation and on the minimization of support interference effects.

SUITABILITY OF HYDROGEN PEROXIDE FOR JET SIMULATION

Study of a number of possible methods of jet simulation led to selection of a monopropellant (hydrogen peroxide) rocket system as being most suitable for the use of the Langley 16-foot transonic tunnel. This system possesses the basic advantages of compactness, small supply lines, and ease of operation (the jet pressure ratio is controlled by simply varying the weight flow through the system (ref. 18)). The products of decomposition of hydrogen peroxide, steam and oxygen, allow safe operation in a wind tunnel. The amount of water added to the airstream would not affect the operation of a large wind tunnel cooled by an air-exchange system although the operation of a hydrogen peroxide jet in a pressurized closed circuit tunnel could increase the dewpoint above tolerable limits.

Physical Properties of Hydrogen Peroxide

Hydrogen peroxide is a clear liquid oxidizer with a high internal energy content. It is used in rocketry in concentrations between 80 and 100 percent (ref. 9). The physical properties of H_2O_2 are listed in references 9 and 19. Some of the physical properties of the mixture of H_2O_2 decomposition products are shown in figure 1. The liquid can be decomposed catalytically by many heavy metals and their salts. The chemical mechanism of hydrogen peroxide decomposition by silver catalyst is discussed in reference 20. Some incomplete decomposition has been experienced with concentrations of hydrogen peroxide lower than 90 percent when using a silver-screen catalyst bed; therefore, only this commercially available concentration was considered. All further reference in this paper to H_2O_2 will mean a concentration of 90 percent by weight, where 90 percent is H_2O_2 and the balance is pure water. Decomposition of 90 percent H_2O_2 results in an increase in volume of 5,233 times with an adiabatic decomposition temperature of 1,364° F at atmospheric pressure. The molecular weight of this gas is 22.105 and the ratio of specific heats γ is 1.266.

Jet Flow Characteristics

It is essential to determine how well the hot exhaust from a hydrogen peroxide jet simulator system will duplicate the shape of a turbine jet. Several typical turbojet-engine operating conditions have been examined

and the important jet parameters for two of these engines installed in fighter airplanes are listed in table I. The geometric parameters for determining the shape of a sonic jet consisting of the decomposition products of 90 percent H_2O_2 exhausting into still air are given in figure 2. These curves have been interpolated for $\gamma = 1.27$ from the charts of reference 12. The charts of reference 12 have also been used to determine the jet-boundary shape parameters for the flight operating conditions of engines A and B (see table I). The shape parameters for the turbojet exhausts and a hydrogen peroxide decomposition jet are compared in table II. Reducing the jet pressure ratio by a few tenths in the jet simulator tests would result in almost identical jet boundaries. In the afterburning case, the initial jet shapes are almost identical; however, the jet temperature is 1,400° to 1,600° F lower with H_2O_2 than that which exists in an afterburning engine tailpipe.

It is interesting to note that a comparison of the kinematic viscosities (part of the Reynolds number, a factor affecting the shear at the jet boundary) of the hydrogen peroxide jet and a turbojet exhaust shows almost perfect agreement. The momentums of the two gases are about the same. The coefficients of thermal conductivity which are involved in the heat transfer between the boundaries are about 10 percent higher for the peroxide jet than those for the turbojet engine. This good agreement of the factors involved in the trailing mixing region indicates that the hydrogen peroxide jet provides adequate simulation of the turbojet-engine exhaust in both the initial jet bulb and in the trailing mixing region.

APPARATUS

The apparatus required for operating a hydrogen peroxide jet simulator system must include suitable storage tanks, a flow-controlling system, and a gas-generator—exit-nozzle combination.

Because of its corrosive nature, special materials must be used for storing and handling concentrated hydrogen peroxide. It can be stored for long periods of time in 99.6 percent pure aluminum containers which have received a special pickling treatment to make the interior surface passive. Certain stainless steels can be used for short-time storage containers by giving them a proper passivation treatment. Reference 21 describes the passivation treatments that can be used on suitable materials. Since hydrogen peroxide is not compatible with many organic and inorganic materials, extreme caution must be used to prevent contact with these materials. Explosive mixtures can be formed with hydrocarbons such as gasoline and alcohol. Reference 21 contains safety precautions for handling and storing hydrogen peroxide. The use of concentrated

H_2O_2 as a propellant requires special equipment and acceptable types are described in references 21 and 22.

Storage and Supply System

Hydrogen peroxide is stored at a tank farm at the Langley 16-foot transonic tunnel which is shown in the photograph of figure 3. The tanks have a capacity of 5,000 gallons each and are constructed of 99.6 percent pure aluminum. The hydrogen peroxide storage system is equipped with temperature monitors and automatic alarm and flooding provisions in case contamination occurs and disposal of the hydrogen peroxide is necessary. The personnel wearing special protective clothing are transferring hydrogen peroxide from the storage field to the supply tank mounted on a trailer.

The trailer-mounted hydrogen peroxide supply system is shown in figure 4. It consists of an 1,100-gallon temporary storage tank, a hydrogen peroxide transfer pump, a 30-gallon high pressure tank, a nitrogen pressurizing cascade, and safety water tank, pump, shower, and hoses. A sketch illustrating the operation of the portable system is presented in figure 5. This trailer is used to transport hydrogen peroxide from railroad tank cars to the storage tank farm and to operate the hydrogen peroxide jet simulators. All transfer and jet supply operations can be controlled from the trailer panel or from a duplicate remote station. Weight flows up to about 7 lb/sec are obtainable at tank pressures up to 1,000 lb/sq in. and are indicated on an electronic flowmeter. The hydrogen peroxide flow rate can be controlled by the amount of pressure on the system and by throttling the flow with a valve. Safety interlocks control the operating sequence and desired flow rates can be established in about 10 seconds by adjusting the throttle valve while observing the flowmeter.

Jet Simulators

The present jet simulator consists of a thrust balance, gas generator, and an exit-nozzle tailpipe. A photograph of a hydrogen peroxide jet simulator is shown in figure 6. Figure 7 shows two designs of these jet simulator units and some of the components are shown in figure 8.

The thrust balances attached to the gas generators were designed to eliminate inlet-momentum corrections of the liquid and Bourdon tube effects and minimize ambient and differential heating effects. During operation of the unit shown in figure 7(a), hot-gas leakage occurred at the O ring seal and the thrust balance experienced excessive zero shifts due to differential temperature effects. The jet simulator was redesigned as shown in figure 7(b) to reduce the internal pressure by eliminating the gas-generator sonic throat. The thrust balance and decomposition

chamber were machined from one block of high-temperature alloy to eliminate welds and a single H_2O_2 passage was provided through the balance. The strain gages were mounted on webs on the sides of the liquid passage and this design improved the accuracy of the thrust measuring system.

The turbojet simulator (fig. 7) utilizes a gas generator which is based on a design obtained from reference 18 and modified for this use. The liquid enters the gas generator at the inlet orifice which is designed to provide a pressure drop of about one-half the chamber pressure at the design flow rate. It has been found that this pressure drop will prevent pressure oscillations called chugging (refs. 7 and 23). The catalyst bed is made up from 20-mesh 0.014-inch-diameter wire screens of 99.6 percent pure silver activated with a samarium nitrate treatment devised by the BECCO Chemical Division. Reference 24 also describes a method for treating catalyst screens with samarium nitrate. The coating treatments in addition to providing faster starts prevent the screens from fusing together under the high temperatures resulting from peroxide decomposition.

These hydrogen peroxide gas-generator units can be made in a wide range of sizes to develop thrust outputs from 2 pounds to 400 pounds and much greater. Figure 9 shows a series of hydrogen peroxide gas-generator units that have been developed for use in research models at the Langley Aeronautical Laboratory of the NACA. They range in size from the small unit (0.5-inch diameter) to the 5.25-inch-diameter unit shown at the top. These units have been developed for wing-tip reaction controls and primary jets in free-flight models, for exhaust simulators in towing-tank seaplane models, for multiengine-jet interference models, for missile rocket-motor simulation, and for the turbojet-engine simulator described herein.

Some of the convergent-nozzle configurations that have been statically tested with the turbojet-engine simulators are shown in figures 6 and 7. These were scaled nonafterburner nozzles corresponding to the turbojet-engine exits listed in table I(a). The exit-nozzle tailpipes shown in figure 7 contained perforated cones; the one in figure 7(a) was a device used to shock the flow to subsonic speed behind the throat and create a large total-pressure loss and the cone was retained in the design shown in figure 7(b) to damp pressure pulses of unknown origin which occurred in the tailpipe.

STATIC TESTS

The hydrogen peroxide jet simulator system was statically tested to determine how the model-exit-nozzle characteristics agreed with those of a turbojet engine nozzle. These tests covered a range of operation

corresponding to that required for a test program of a transonic wind-tunnel model.

The instrumentation used during the static tests consisted of a thrust balance, total-pressure and static-pressure orifices located in the gas generator and exit-nozzle tailpipe, and thermocouples located both inside the jet simulator and on the outside surface of the unit. Pressures were measured with electrical transducers and transmitted through carrier amplifiers to recording oscillographs. Thrust-balance strain-gage output was also measured on the recorder. Temperature measurements were obtained on multichannel or pen-trace self-balancing potentiometers. All tests were made by varying the flow rate of H_2O_2 through the jet simulator system in predetermined steps of 10 to 20 seconds duration.

The estimated accuracy of the pressure measurements is ±3 percent. Thrust measurements presented herein were obtained on the second design (fig. 7(b)) and are estimated to be within 1 percent of full scale or about ±4 pounds of thrust.

Internal Pressures

The first step in investigating the operation of the turbojet simulator was to determine if the design condition of a sonic exit had been met. Figure 10 shows the distribution of internal pressures along the walls of the turbojet simulator. The circle symbols are data taken with no shock inducing devices in the tailpipe. The steady increase in static pressure at the walls downstream of what is apparently a strong supersonic compression and the decrease in total pressure in the passage is an indication of a series of oblique shocks in supersonic flow. The flow did not shock to subsonic speed until beyond the orifice at the 15.2 station and supersonic flow persisted through the entire tailpipe for decomposition-chamber pressures slightly higher than those presented. It was decided, therefore, to install some heavy wire screens in the tailpipe. The results with two screens showed that the flow shocked to subsonic speeds just behind the second screen and accelerated to a Mach number of 1.0 at the exit nozzle. The rapid-heat cycling and pressure changes produced by short runs soon caused failure of the heavy wire screens; therefore, perforated cones (fig. 8) were designed as shock inducing devices. Tests with a cone shown in figure 10 (square and diamond symbols) indicated that the perforated cone produced the desired subsonic flow. The solid line on the Mach number distribution indicates the values that would be obtained from the area distribution. Sonic exit conditions with the perforated cone were obtained at all pressure ratios above that required to choke the nozzle.

A multiple-tube total-pressure rake was installed in a simulator exit-nozzle tailpipe at about the 16.7-inch station. The radial survey of the total-pressure distribution for several values of jet total-pressure ratio, $p_{t,j}/p_0$, based on center-line tube reading is shown in figure 11. These results indicate that the total pressure distribution is quite flat across the section, except at the highest pressure ratios. In addition, it appears that the boundary layer is relatively thin and is expected to remain so as the flow accelerates to the exit nozzle.

Temperature Surveys

The variation of temperature, both internally and externally, along the jet simulator is shown in figure 12, at the locations indicated in the top sketch. Internal total temperatures were measured with liquid or stagnation-type thermocouples having a high-temperature recovery factor. The distribution of the temperature rise through the catalyst bed is unknown, but a temperature increase of 1,320° F occurred from the void space ahead of the catalyst to the chamber measurement in back of the bed. Discoloration of the steel of the decomposition chamber indicates that most of the temperature increase occurs in the initial one-third of the bed. The temperature losses through the walls of this tailpipe were small; a decomposition temperature of 1,385° F was measured behind the catalyst bed and the stagnation temperature dropped 35° F to a value of 1,350° F at the exit measuring station. The fact that the measured decomposition temperature was higher than the theoretical value of 1,364° F for 90 percent hydrogen peroxide may be the result of higher H_2O_2 concentration, higher than standard inlet temperature and decomposition chamber pressure. Skin temperatures show a more gradual rise, reaching a maximum of 1,100° F at 15 inches from the inlet to the decomposition chamber. It should be pointed out that the temperature variation shown exists while peroxide is being decomposed in the system. Upon shut-off, skin temperatures on the tailpipe will decrease, but the temperatures at the upstream end of the decomposition chamber will increase as the heat flows back into the inlet system which has been cooled by the liquid peroxide during jet operation. The temperatures of the connecting end of the thrust balance may approach 250° F which represents a limit for strain-gage installations. It is apparent that the residual heat of the jet simulator may be a problem when the unit is installed inside a model near instrumentation.

Flow Measurements

Static tests with atmospheric back pressure have been conducted on the jet simulator systems shown in figure 7. Weight-flow measurements obtained from the liquid hydrogen peroxide flowmeter are compared in

figure 13 with calculated flow rates at the two jet-simulator sonic nozzles shown in figure 7(a). The total pressure and temperature measured in the decomposition chamber and in the tailpipe were used to determine the flow rates at the throat and exit, respectively. Calculations for the d_j = 3.20-inch nozzle are not shown below a primary weight flow of 2.0 lb/sec, since the jet was not choked in this region. The measurements of the weight flow taken at the three different points in the system are shown to be in good agreement.

Weight-flow data for tailpipes with the throat removed (fig. 7(b)) and some data repeated from figure 13 are compared with liquid flowmeter measurements in figure 14. From these data, discharge coefficients, C_d, defined as the ratio of measured to theoretical weight flow calculated from the exhaust-gas measurements, have been determined. The average value of the discharge coefficient for these convergent nozzles is about 0.97, which is consistent with usual convergent-nozzle values (for example, refs. 25 and 26). This correspondence is an indication of uniform flow across the exit nozzle.

The relationship between propellant weight flow and jet pressure ratio for various sizes of convergent nozzles with a hydrogen peroxide jet simulator system is shown in figure 15. The solid lines represent the ideal relationship for the decomposition products of 90 percent hydrogen peroxide calculated for the adiabatic decomposition temperature of 1,364° F and standard atmospheric conditions. The linear variation of jet pressure ratio with weight flow of propellant is illustrated for sonic nozzle conditions. In the actual case, the nozzle would not be choked below the critical total to static pressure ratio of 1.82 for γ = 1.27, and all the curves would fair into a jet-off pressure ratio of 1.0 since the flow is zero at this point. The test points shown (d_j = 2.62 in.) are measurements of the liquid hydrogen peroxide flow rate obtained from the electronic flowmeter. Calculated weight flows determined from measured exhaust-gas pressures and temperatures are compared with the flowmeter measurements. The deviation of this calculated flow from the ideal values is due to using the measured jet temperature which was lower than the adiabatic decomposition temperature and to a higher ambient pressure than standard.

The decomposition chamber was designed for a weight flow of 4 lb/sec using the specific flow rate of 0.333 lb/sec/in.^{2} of cross-sectional area (ref. 18) and the unit could pass weight flows up to 7 lb/sec with smooth and steady operation, with instant starts and stops being made once the propellant lines were filled. It has been found that for the size of the decomposition chamber and the flow rates used (average flow rate 2.5 lb/sec) the catalyst bed would last for about 1 hour before the bed deteriorated. The bed life cannot be accurately predicted for other

units because many of the factors affecting the life are unknown. With the exit nozzle shown in figure 7(b) (d_j = 2.62 in.), jet total to ambient pressure ratios up to 5 could be easily established in the static test facility. It should be noted that pressure ratios of 10 will probably be obtained in the Langley 16-foot transonic tunnel inasmuch as the free-stream static pressure drops to about one-half atmosphere at a Mach number of 1.0. This pressure ratio is about twice that required for turbojet-engine operation (ref. 27) in the speed range available in this transonic tunnel.

Thrust Measurements

The variation of jet thrust with pressure ratio is presented in figure 16 for a convergent nozzle having an exit diameter of 3.20 inches. Measured thrust is compared with the ideal convergent nozzle thrust and the ideal thrust for complete isentropic expansion of the nozzle flow. The ideal thrusts have been calculated from measured weight flows, jet total temperatures and jet total pressures. The ratio of measured jet thrust to the ideal thrust for complete isentropic expansion is also shown in this figure and has an average value of about 0.97 for this nozzle.

The variation of static thrust coefficient $C_{F,0}$ with jet pressure ratio is presented in figure 17 for three convergent nozzles. The static thrust coefficient nondimensionalizes the data so that all sizes of nozzles should be on a single line. The differences between the nozzles are mainly due to differences in the nozzle discharge coefficients. The data presented in figures 16 and 17 indicate that the thrust values obtained with the jet simulator are in good agreement with the theoretical values for full-scale convergent nozzles (ref. 28).

CONCLUDING REMARKS

A hydrogen peroxide turbojet-engine exhaust simulator for powered-model testing in wind tunnels with air exchange has been developed. The hydrogen peroxide system provides a hot jet whose characteristics correspond closely to the exhaust of a turbojet engine. This system has the advantage of compactness, small propellant lines, and simple control over the jet pressure ratio by varying the propellant flow rate. The necessary associated equipment needed to operate the system has been described. Static-test data obtained with the hydrogen peroxide system show that experimental results with convergent nozzles are in good

agreement with theoretical values and consistent with convergent-nozzle discharge and thrust coefficients.

Langley Aeronautical Laboratory,
National Advisory Committee for Aeronautics,
Langley Field, Va., July 29, 1957.

REFERENCES

1. Cortright, Edgar M., Jr., and Schroeder, Albert H.: Investigation at Mach Number 1.91 of Side and Base Pressure Distributions Over Conical Boattails Without and With Jet Flow Issuing From Base. NACA RM E51F26, 1951.

2. Cortright, Edgar M., Jr., and Kochendorfer, Fred D.: Jet Effects on Flow Over Afterbodies in a Supersonic Stream. NACA RM E53H25, 1953.

3. De Moraes, Carlos A., Hagginbothom, William K., Jr., and Falanga, Ralph A.: Design and Evaluation of a Turbojet Exhaust Simulator, Utilizing a Solid-Propellant Rocket Motor, for Use in Free-Flight Aerodynamic Research Models. NACA RM L54I15, 1954.

4. Henry, Beverly Z., Jr., and Cahn, Maurice S.: Preliminary Results of an Investigation at Transonic Speeds To Determine the Effects of a Heated Propulsive Jet on the Drag Characteristics of a Related Series of Afterbodies. NACA RM L55A24a, 1955.

5. Cubbage, James M., Jr.: Jet Effects on the Drag of Conical Afterbodies for Mach Numbers of 0.6 to 1.28. NACA RM L57B21, 1957.

6. Pel, C., and Rustemeyer, A.: Investigation of Turbojet Exhaust-Interference Drag. Rep. R-0801-12., United Aircraft Corp. Res. Dept., Nov. 1955.

7. Tormey, J. F.: Experimental Operation of a Gas Generator Utilizing the Hydrogen Peroxide and Cobalt-Plated Screen-Type Catalyst System. Rep. No. AL-815, North American Aviation, Inc., Dec. 27, 1948.

8. Sutton, George P.: Rocket Propulsion Elements. Second ed., John Wiley & Sons, Inc., c.1956, pp. 273-276.

9. Bloom, Ralph, Jr., Davis, Noah S., Jr., and Levine, Samual D.: Hydrogen Peroxide as a Propellant. Jour. American Rocket Soc., no. 80, Mar. 1950, pp. 3-17.

10. Draley, Eugene C.: Experience With Some Special Techniques in Transonic Wind Tunnels of the NACA-Langley Laboratory. Proceedings of the Propulsion Wind Tunnel Transonic Seminar. Vol. II. Discussion of Transonic Wind Tunnel Operational Problems. Arnold Eng. Dev. Center, U.S.A.F. Air Res. and Dev. Command, July 23-25, 1956.

11. Li, T. Y., Yoler, Y. A., and Morgan, A. J. A.: The Design of Wind Tunnel Experiments for the Study of Jet-On Effects. NAVORD Rep. 3473 (NOTS 1081), U.S. Naval Ord. Test Station (China Lake, Calif.), Apr. 12, 1955.

12. Love, Eugene S., and Grigsby, Carl E.: Some Studies of Axisymmetric Free Jets Exhausting From Sonic and Supersonic Nozzles Into Still Air and Into Supersonic Streams. NACA RM L54L31, 1955.

13. Henry, Beverly Z., Jr., and Cahn, Maurice S.: Additional Results of an Investigation at Transonic Speeds To Determine the Effects of a Heated Propulsive Jet on the Drag Characteristics of a Series of Related Afterbodies. NACA RM L56G12, 1956.

14. Bressette, Walter E.: Some Experiments Relating to the Problem of Simulation of Hot Jet Engines in Studies of Jet Effects on Adjacent Surfaces at a Free-Stream Mach Number of 1.80. NACA RM L56E07, 1956.

15. Swihart, John M., and Crabill, Norman L.: Steady Loads Due to Jet Interference on Wings, Tails, and Fuselages at Transonic Speeds. NACA RM L57D24b, 1957.

16. Kochendorfer, Fred D.: Effect of Properties of Primary Fluid on Performance of Cylindrical Shroud Ejectors. NACA RM E53L24a, 1954.

17. Wallner, Lewis E., and Jansen, Emmert T.: Full-Scale Investigation of Cooling Shroud and Ejector Nozzle for a Turbojet Engine - Afterburner Installation. NACA RM E51J04, 1951.

18. McCormick, James C., and Bloom, Ralph, Jr.: Design for an Improved H_2O_2 Decomposition Chamber for the LR8-RM6 Rocket Engines. Eng. Rep. LR-E1 (Contracts NOas 52-779-c and NOas 53-1034-c), Food Machinery and Chemical Corp., Buffalo Electro-Chemical Company, Inc., June 1953.

19. Anon.: Hydrogen Peroxide Physical Properties Data Book. Second ed. Bull. No. 67, Food Machinery and Chemical Corp., BECCO Chemical Div. (Buffalo), 1955.

20. Wentworth, R. L.: The Mechanism of the Catalytic Decomposition of Hydrogen Peroxide by Silver. Rep. No. 32, D.I.C. 6552 (Contract No. N5ori-07819), M.I.T., May 1, 1951.

21. Anon.: Handbook - Field Handling of Concentrated Hydrogen Peroxide (Over 52 Weight Percent Hydrogen Peroxide). NAVAER 06-25-501, Bur. Aero., July 1, 1955. (Rev. Jan. 15, 1957.)

22. Davis, Noah S., Jr., and Keefe, John H., Jr.: Equipment for Use With High-Strength Hydrogen Peroxide. Jour. American Rocket Soc., vol. 22, no. 2, Mar.-Apr. 1952, pp. 63-69.

23. Hunter, W., and Sherwood, B. J.: Report on Development of the Gas Generator for the XLR43-NA-1 Rocket Propulsion System. Rep. No. AL-1195, North American Aviation, Inc., Feb. 1, 1951.

24. Moore, G. E., Driscoll, D. H., and Berman, K.: A Hybrid Rocket Propellant System: 90-Percent Hydrogen Peroxide - Solid Fuel. Rep. No. R53A0509, Project HERMES (Contract No. DA-30-115-ORD-23), General Electric, July 1954.

25. Beale, William T., and Povolny, John H.: Internal Performance of Two-Dimensional Wedge Exhaust Nozzles. NACA RM E56K29b, 1957.

26. Huntley, S. C., and Yanowitz, Herbert: Pumping and Thrust Characteristics of Several Divergent Cooling-Air Ejectors and Comparison of Performance With Conical and Cylindrical Ejectors. NACA RM E53J13, 1954.

27. Cortright, Edgar M., Jr.: Some Aerodynamic Considerations of Nozzle-Afterbody Combinations. Aero. Eng. Rev., vol. 15, no. 9, Sept. 1956, pp. 59-65.

28. Greathouse, W. K.: Preliminary Investigation of Pumping and Thrust Characteristics of Full-Size Cooling-Air Ejectors at Several Exhaust-Gas Temperatures. NACA RM E54A18, 1954.

TABLE I

TYPICAL TURBOJET-ENGINE CONDITIONS FOR FIGHTER AIRCRAFT

(a) Cruise flight

Turbojet engine	A	B
Maximum sea-level nonafterburning thrust	9,220	7,600
Mach number	0.80	0.90
Altitude, ft	35,000	42,000
Power, percent of maximum thrust at altitude	50	65
Cruise thrust, lb	1,612	1,040
Thrust coefficient, C_F	0.0310	0.0206
Primary air flow, lb/sec	54.4	34.5
Secondary flow ratio, $w_s/w_p\sqrt{T_{t,s}/T_{t,p}}$	0	0.059
Fuel-air ratio	0.008	0.012
Jet temperature, $^{\circ}R$	1,020	1,060
Jet temperature ratio, $T_{t,j}/T_{\infty}$	2.59	2.69
Jet total-pressure ratio, $p_{t,j}/p_{\infty}$	2.75	3.10
Jet static-pressure ratio, p_j/p_{∞}	1.43	1.64
Jet density ratio, ρ_j/ρ_{∞}	0.654	0.721
Jet velocity, V_j, ft/sec	1,423	1,475
Jet velocity ratio, V_j/V_{∞}	1.775	1.685
Jet Mach number ratio, M_j/M_{∞}	1.25	1.11
Jet weight-flow ratio, w_j/w_{∞}	1.20	1.22
Exhaust ratio of specific heats, γ	1.374	1.383
Exhaust-gas constant, R	53.40	53.35
Jet γ ratio, γ/γ_{∞}	0.982	0.988
Primary-nozzle diameter, d_j, in.	22.5	19.6

TABLE I.- Continued

TYPICAL TURBOJET-ENGINE CONDITIONS FOR FIGHTER AIRCRAFT

(b) Military power flight

Turbojet engine	A	B
Maximum sea-level nonafterburning thrust	9,220	7,600
Mach number	0.90	1.00
Altitude, ft	35,000	35,000
Power, percent of maximum thrust at altitude	100	100
Cruise thrust, lb	3,133	2,900
Thrust coefficient, C_F	0.0301	0.034
Primary air flow, lb/sec	76.2	60
Secondary flow ratio, $w_s/w_p\sqrt{T_{t,s}/T_{t,p}}$	0	0.06
Fuel-air ratio	0.013	0.016
Jet temperature, $^{\circ}R$	1,400	1,585
Jet temperature ratio, $T_{t,j}/T_{\infty}$	3.56	4.02
Jet total-pressure ratio, $p_{t,j}/p_{\infty}$	4.53	4.2
Jet static-pressure ratio, p_j/p_{∞}	2.50	2.25
Jet density ratio, ρ_j/ρ_{∞}	0.630	0.679
Jet velocity, V_j, ft/sec	1,630	1,762
Jet velocity ratio, V_j/V_{∞}	1.86	1.81
Jet Mach number ratio, M_j/M_{∞}	1.11	1.00
Jet weight-flow ratio, w_j/w_{∞}	1.59	1.24
Exhaust ratio of specific heats, γ	1.346	1.33
Exhaust-gas constant, R	53.45	53.42
Jet γ ratio, γ/γ_{∞}	0.961	0.986
Primary-nozzle diameter, d_j, in.	22.5	19.6

TABLE I.- Concluded

TYPICAL TURBOJET-ENGINE CONDITIONS FOR FIGHTER AIRCRAFT

(c) Afterburner climb and acceleration

Turbojet engine	A	B
Maximum sea-level afterburning thrust	14,000	11,000
Mach number	0.90	0.93
Altitude, ft	35,000	35,000
Power, percent of maximum thrust at altitude	100	100
Thrust, lb	5,955	4,850
Thrust coefficient, C_F	0.0572	0.057
Primary air flow, lb/sec	78.4	56.1
Secondary flow ratio, $w_s/w_p\sqrt{T_{t,s}/T_{t,p}}$	0	0.06
Fuel-air ratio	0.052	0.050
Jet temperature, $^{\circ}R$	3,220	3,600
Jet temperature ratio, $T_{t,j}/T_{\infty}$	8.18	9.14
Jet total-pressure ratio, $p_{t,j}/p_{\infty}$	4.47	3.90
Jet static-pressure ratio, p_j/p_{∞}	2.47	2.17
Jet density ratio, ρ_j/ρ_{∞}	0.336	0.293
Jet velocity, V_j, ft/sec	2,488	2,640
Jet velocity ratio, V_j/V_{∞}	2.84	2.92
Jet Mach number ratio, M_j/M_{∞}	1.11	1.076
Jet weight-flow ratio, w_j/w_{∞}	0.999	1.000
Exhaust ratio of specific heats, γ	1.274	1.27
Exhaust-gas constant, R	53.62	53.60
Jet γ ratio, γ/γ_{∞}	0.910	0.907
Primary-nozzle diameter, d_j, in.	27.0	24.8

TABLE II

BOUNDARY-SHAPE PARAMETERS FOR THE TURBOJET EXHAUST AND HYDROGEN PEROXIDE JETS

(a) Cruise flight

	Engine A	H_2O_2	Engine B	H_2O_2
$p_{t,j}/p_\infty$	2.7	2.7	3.1	3.1
γ	1.37	1.27	1.38	1.27
δ	7	7.2	8.5	10.2
r/d_j	6	5.9	5	4.6

(b) Military power flight

	Engine A	H_2O_2	Engine B	H_2O_2
$p_{t,j}/p_\infty$	4.53	4.53	4.20	4.20
γ	1.346	1.27	1.33	1.27
δ	17.2	18.8	15.7	17.0
r/d_j	3.55	3.50	3.75	3.65

(c) Afterburner climb and acceleration

	Engine A	H_2O_2	Engine B	H_2O_2
$p_{t,j}/p_\infty$	4.47	4.47	3.90	3.90
γ	1.274	1.27	1.27	1.27
δ	18.2	18.5	15.6	15.6
r/d_j	3.53	3.52	3.80	3.80

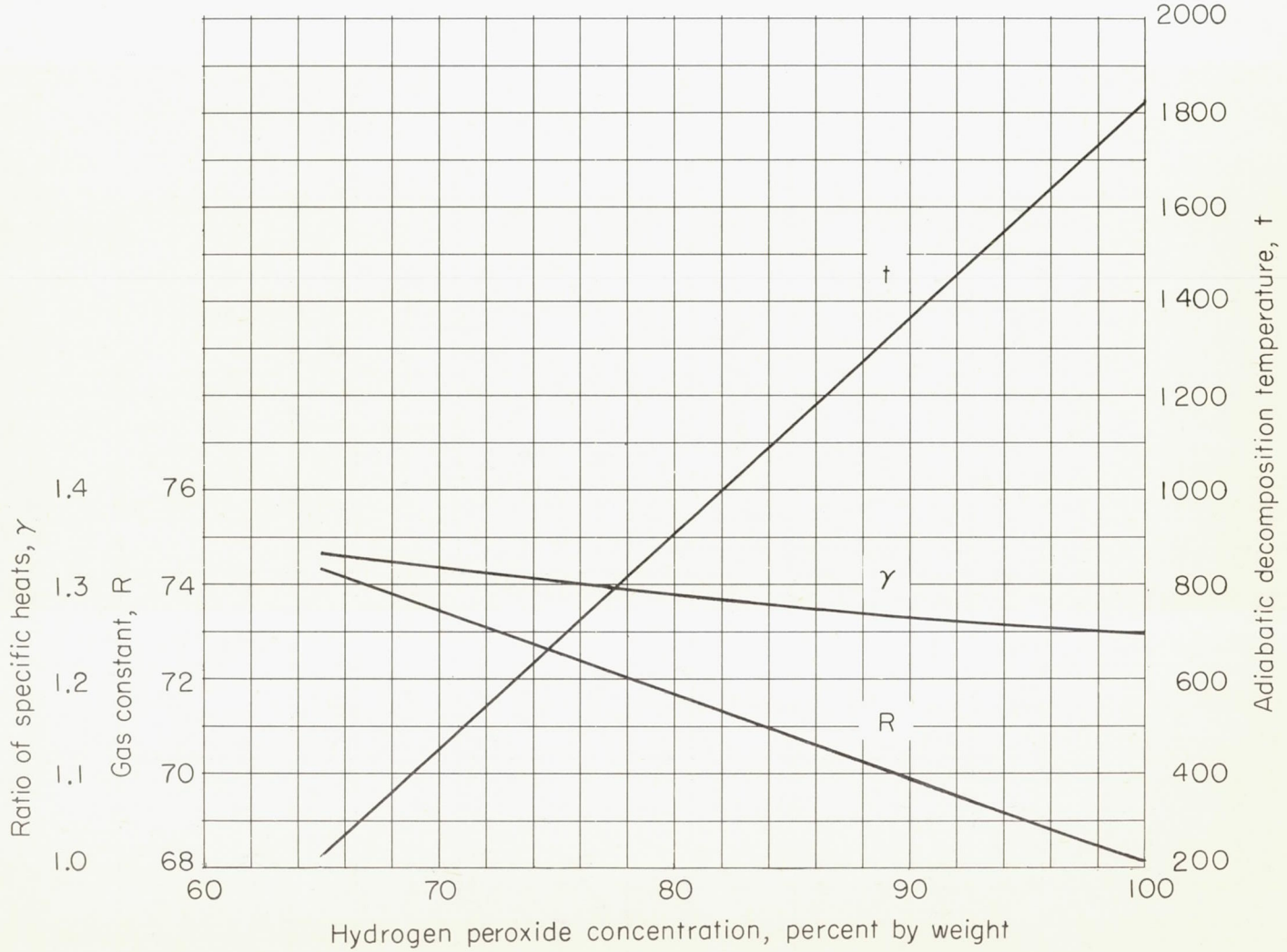


Figure 1.- Physical properties of hydrogen peroxide decomposition products. Adiabatic decomposition of unconfined system at 1.0 atmosphere.

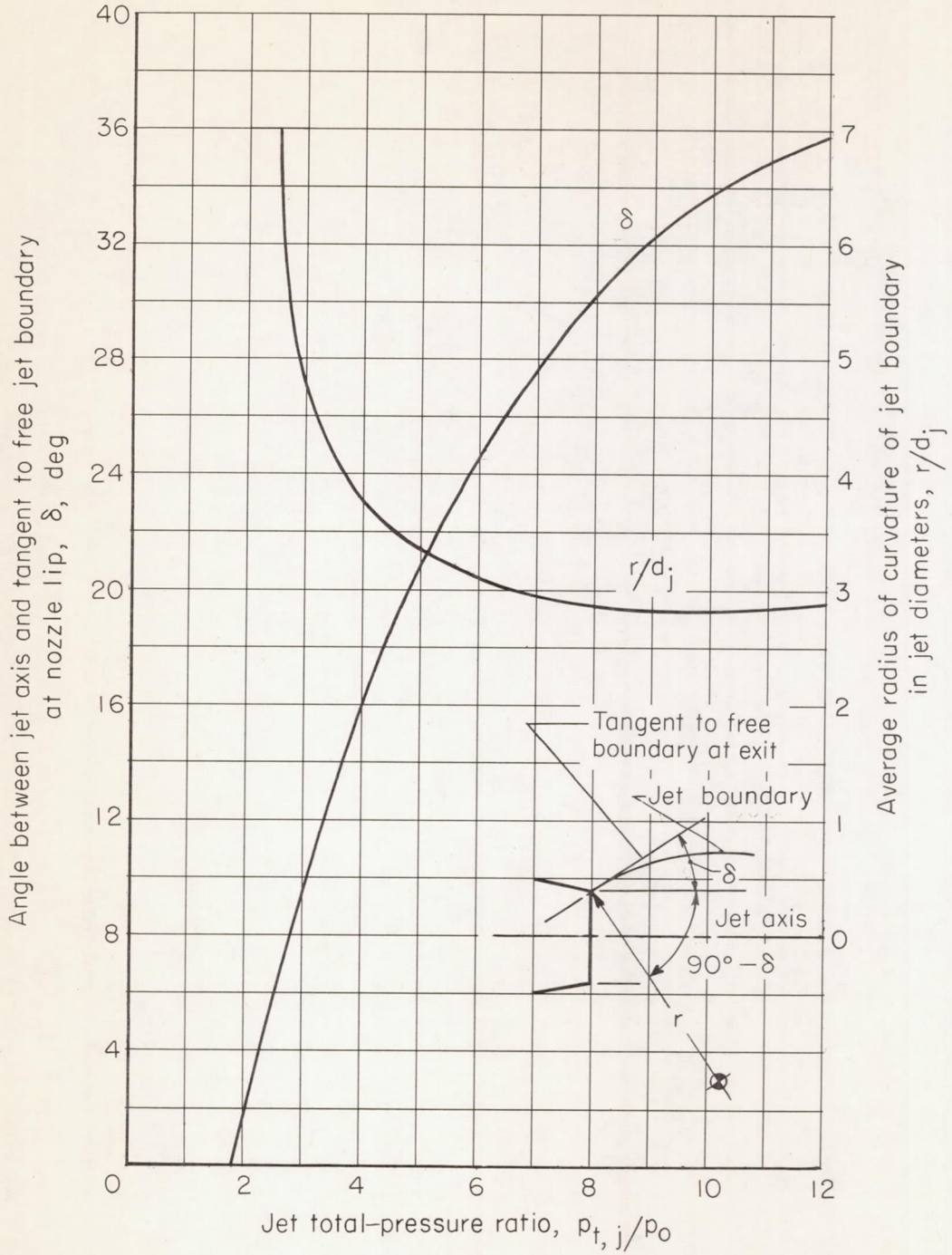
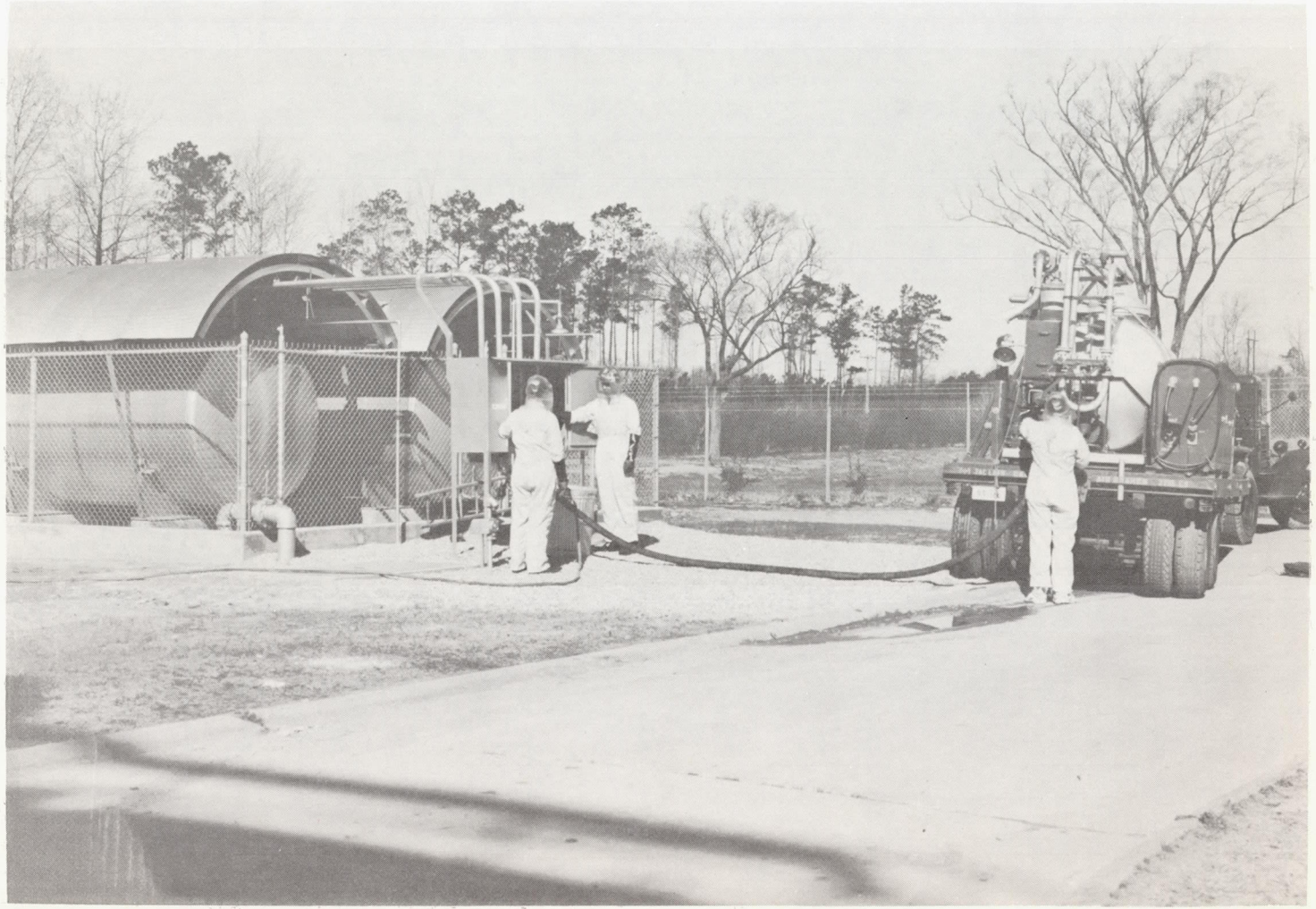


Figure 2.- Jet-boundary shape parameters for 90 percent by weight hydrogen peroxide decomposition products. Convergent nozzle exhausting into still air. $M_j = 1.0$; $\gamma = 1.27$.



L-88693

Figure 3.- Hydrogen peroxide storage tanks and portable supply system.

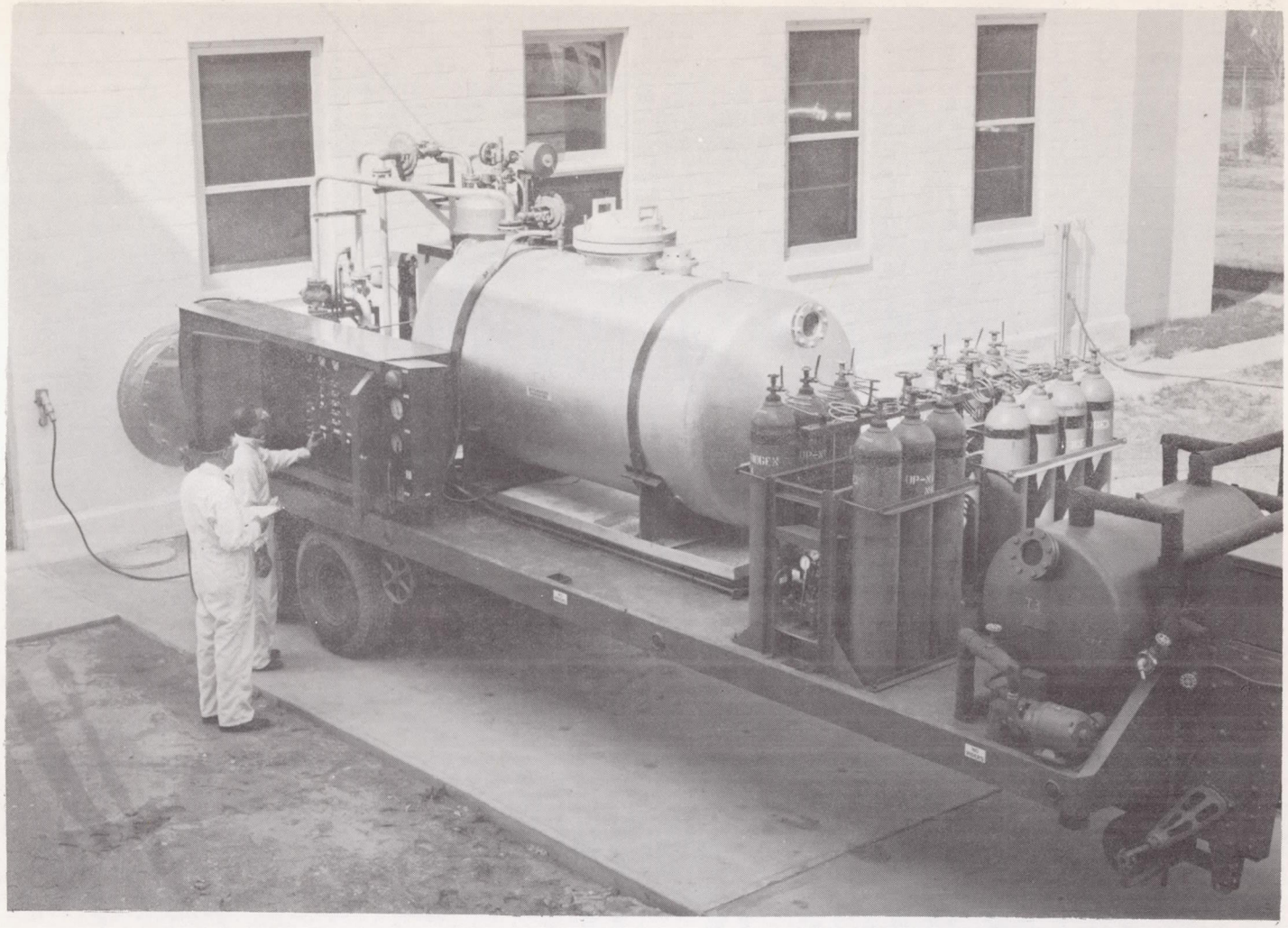


Figure 4.- Trailer-mounted hydrogen peroxide supply system. L-88783

OPERATION

1. Pump H_2O_2 from storage tank to vented high-pressure tank
2. Close vent; pressurize 30-gallon tank with nitrogen
3. Open run valve and set throttle valve for proper flow rate for desired pressure ratio
4. When flow has stabilized at required pressure ratio (5 sec), take data record (5 sec)
5. Repeat step 4 for other pressure ratios
6. Close run valve

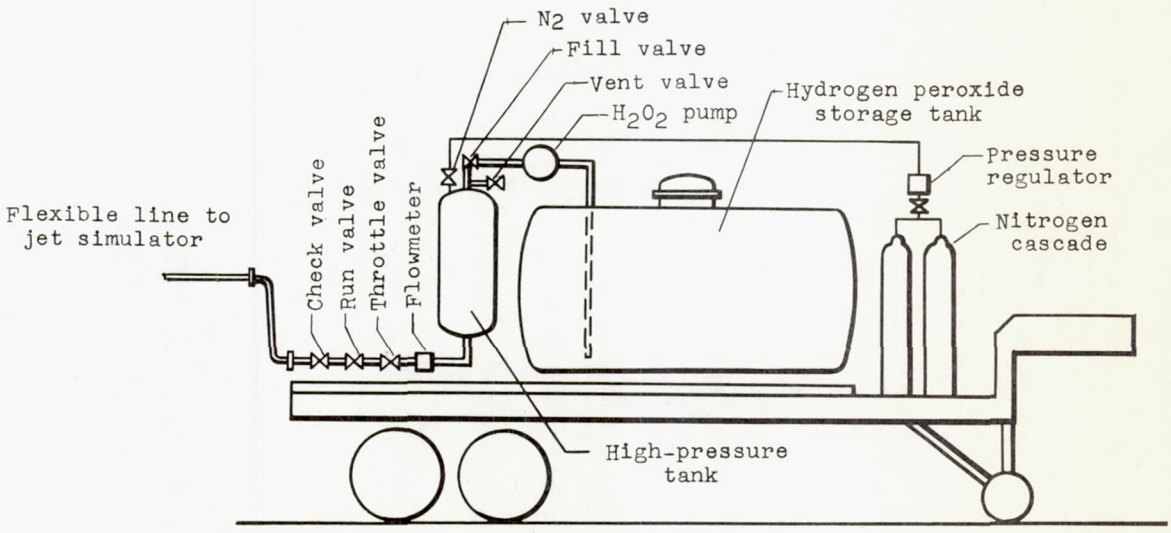


Figure 5.- Schematic sketch of the hydrogen peroxide portable supply system and operating sequence.

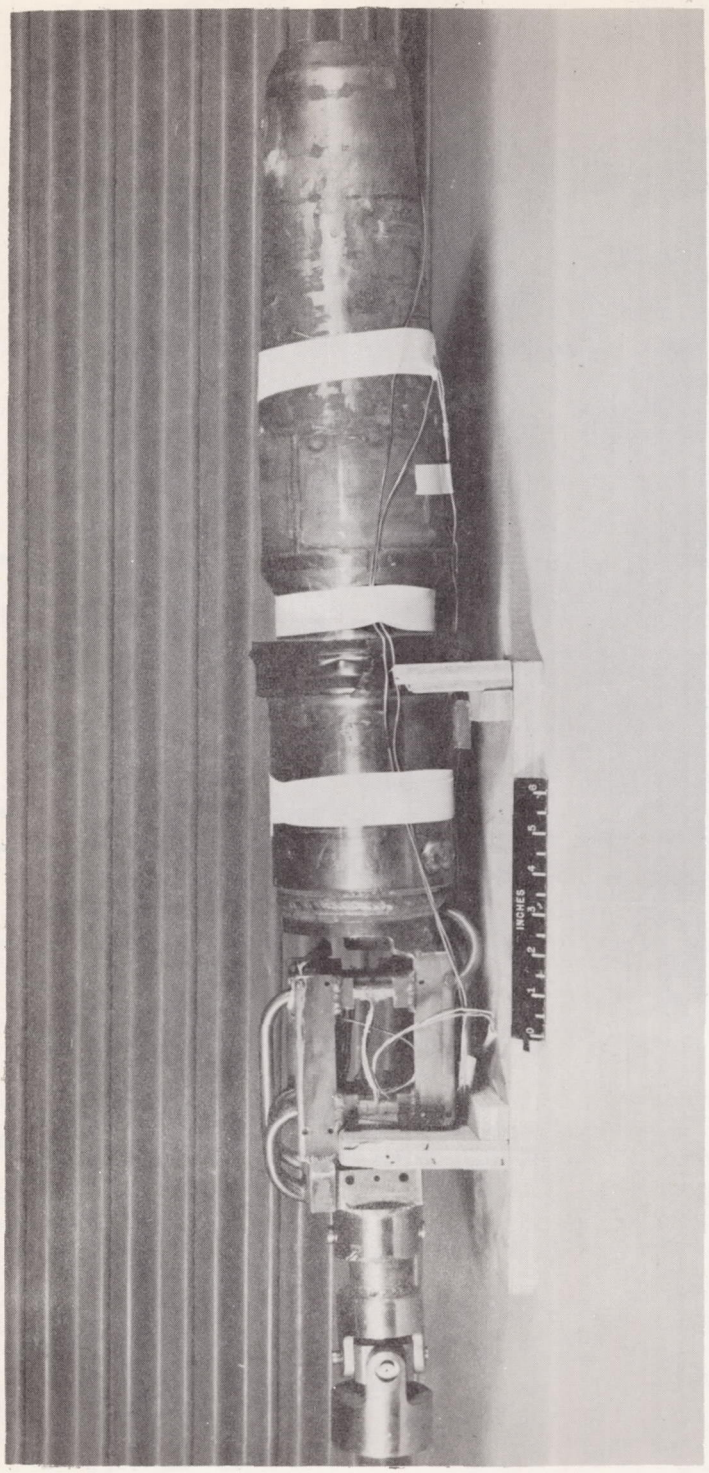
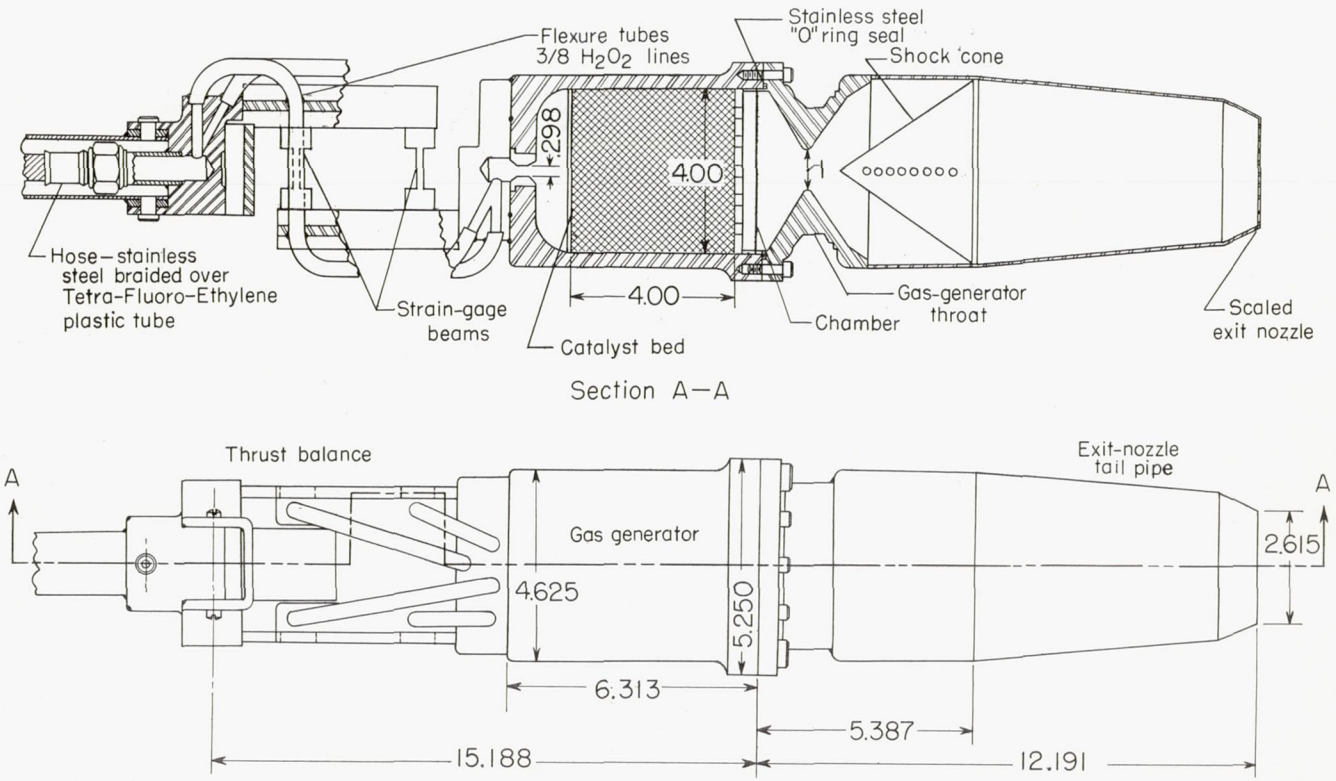
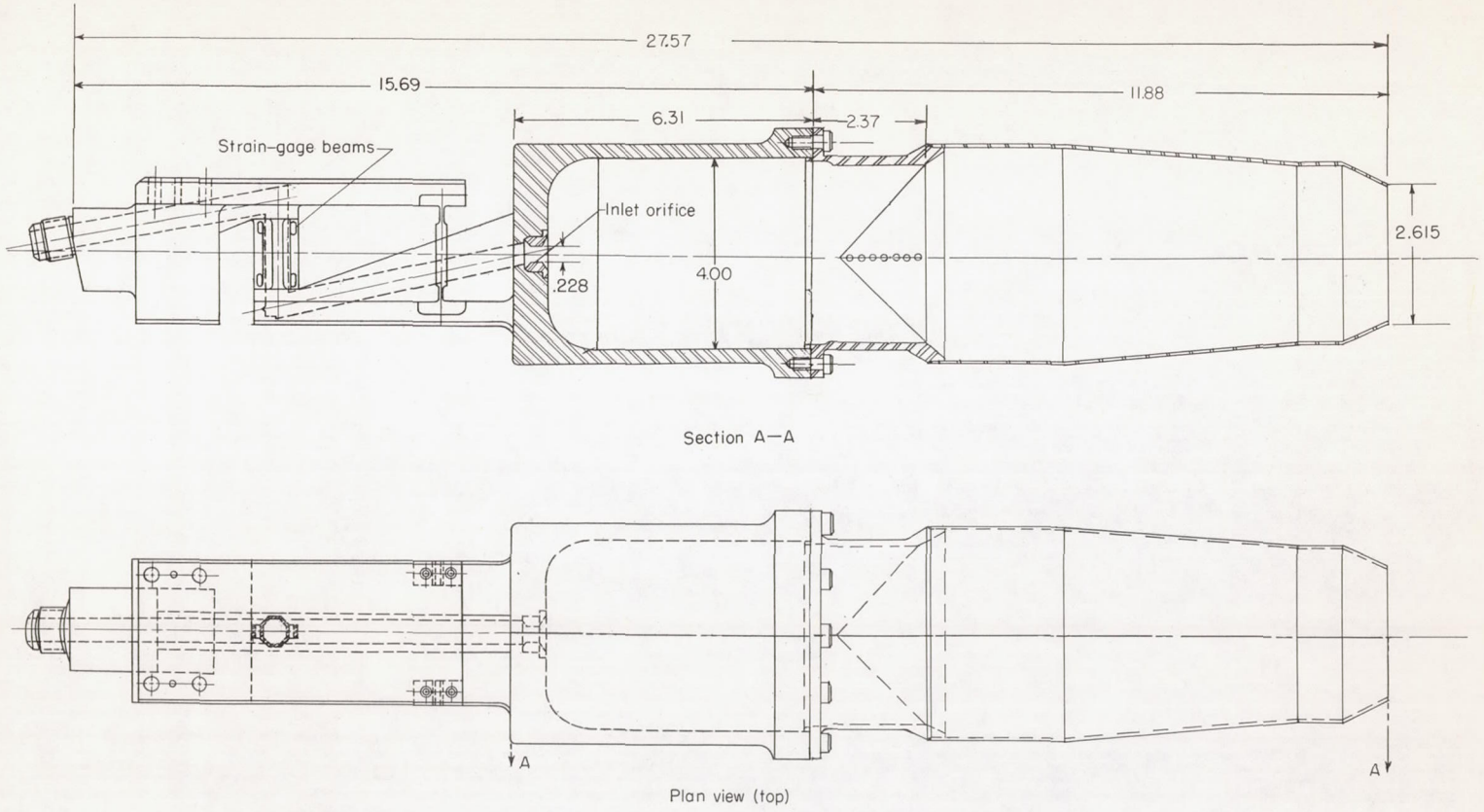


Figure 6.- Photograph of hydrogen peroxide jet simulator. L-96666



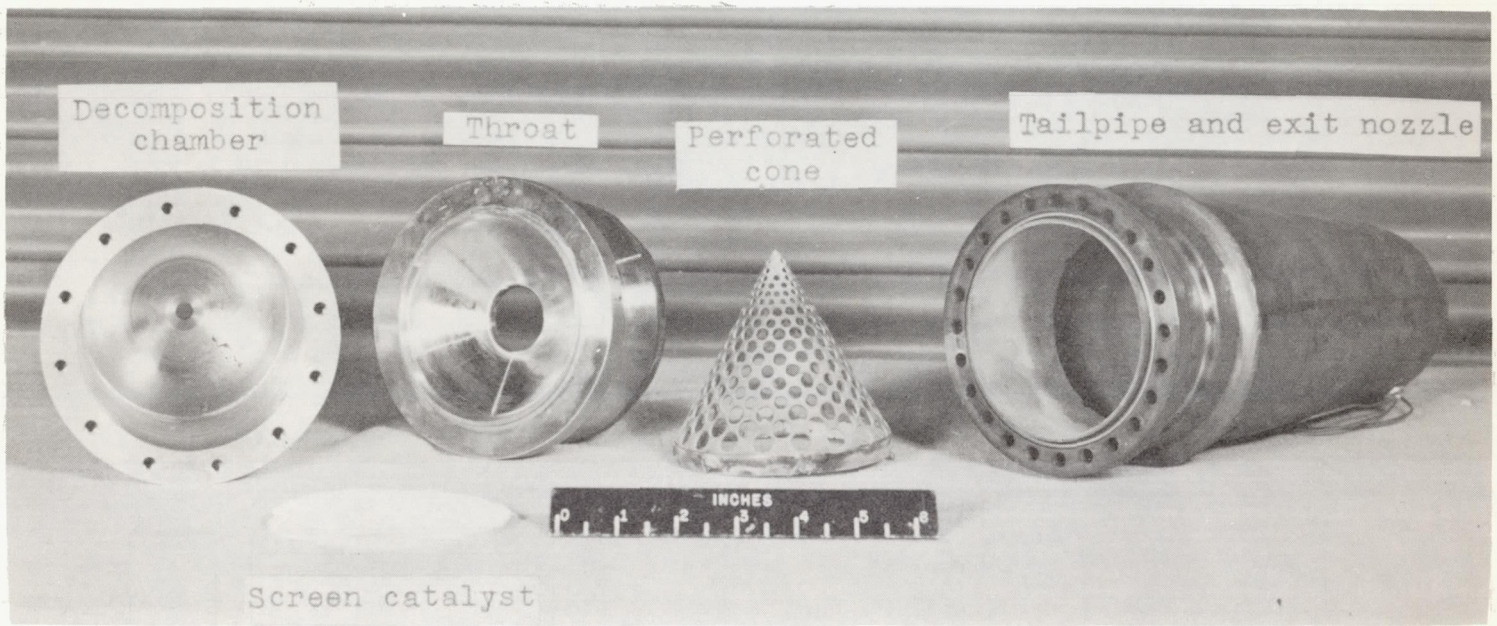
(a) First design.

Figure 7.- Details of hydrogen peroxide gas-generator thrust balance system. (All dimensions are in inches.)



(b) Second design.

Figure 7.- Concluded.



L-96668.1

Figure 8.- Photograph of components of the gas-generator—tailpipe system.

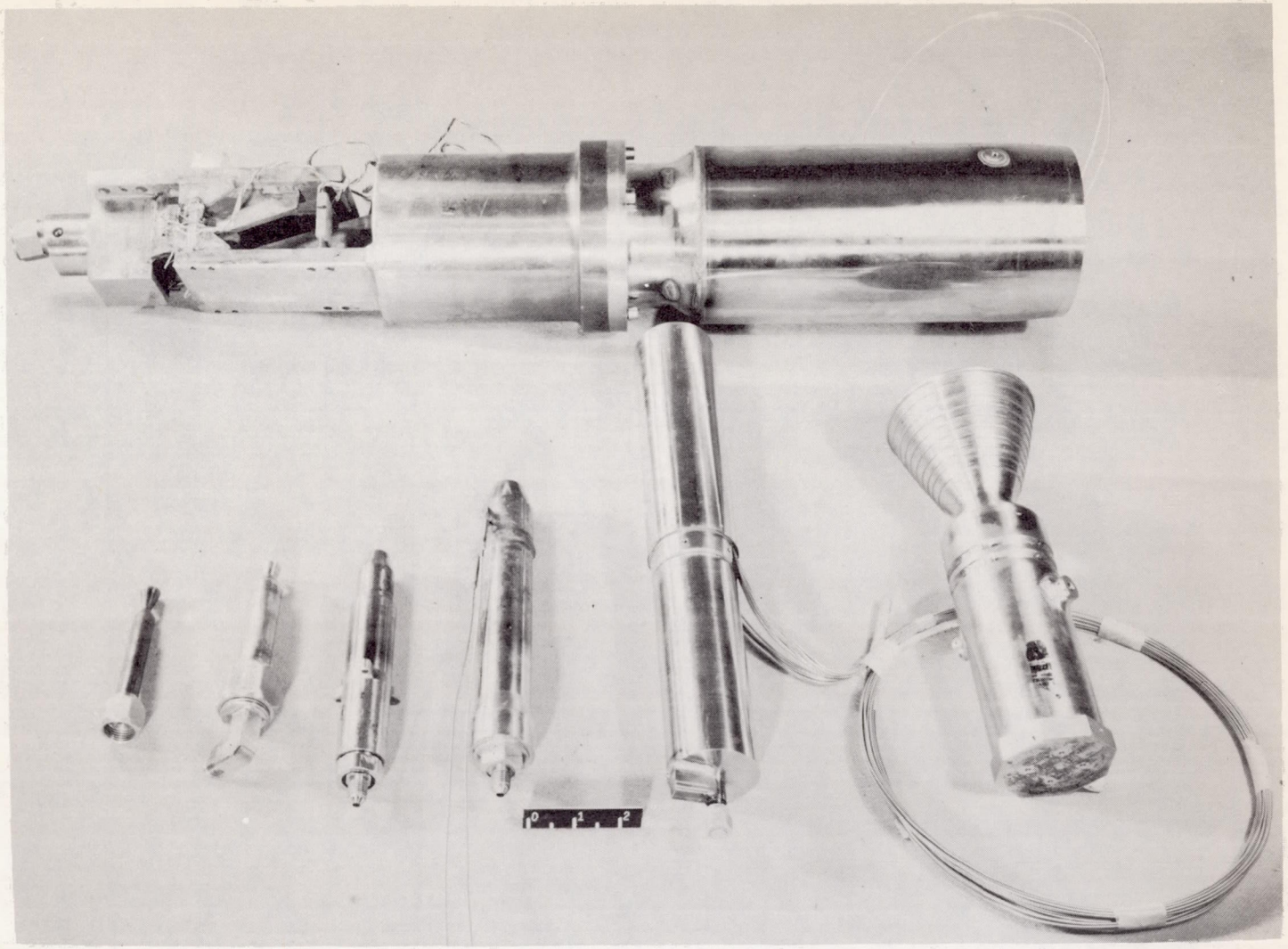


Figure 9.- Hydrogen peroxide gas-generator units. L-57-2561

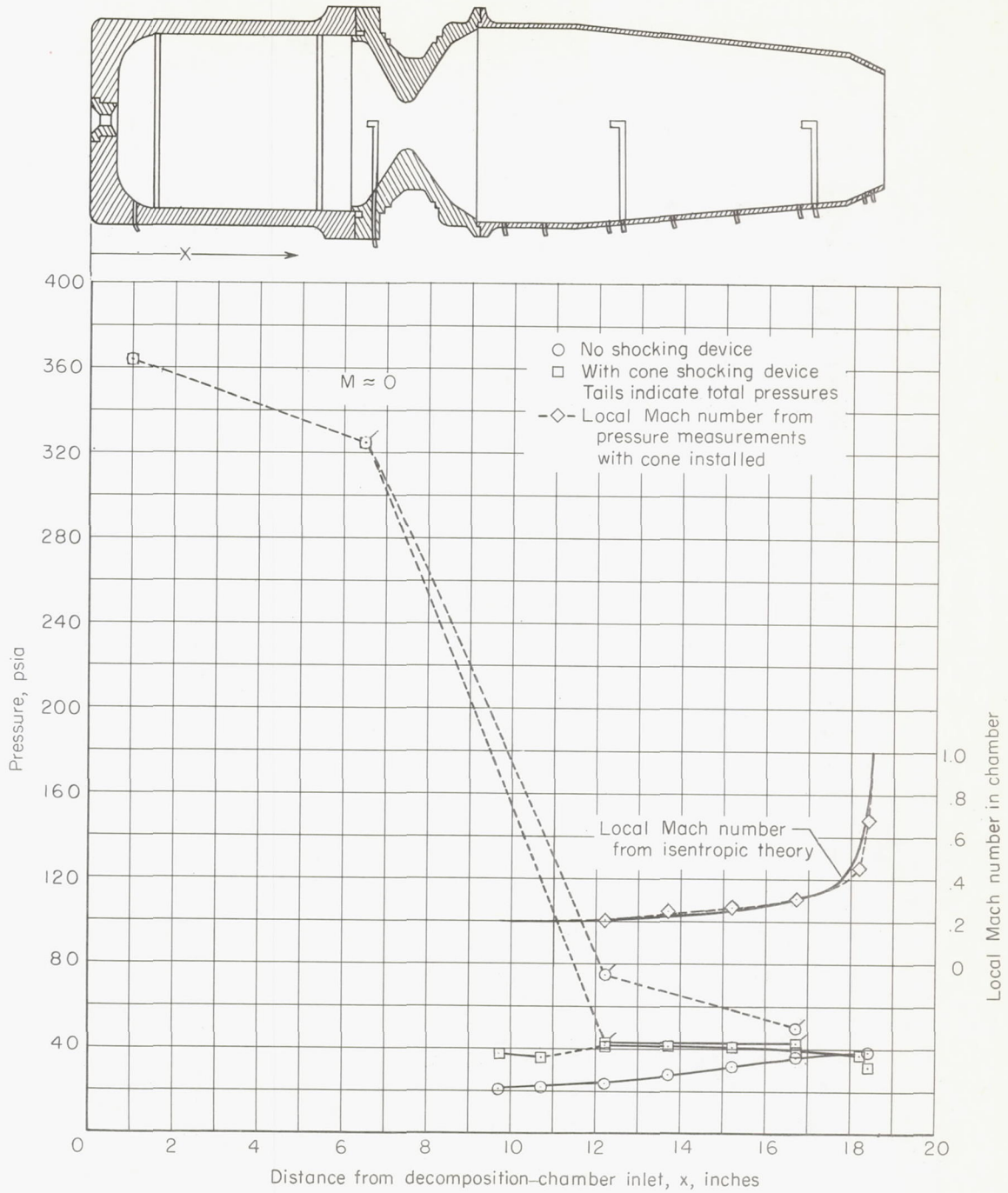


Figure 10.- Variation of measured internal pressure along jet simulator.

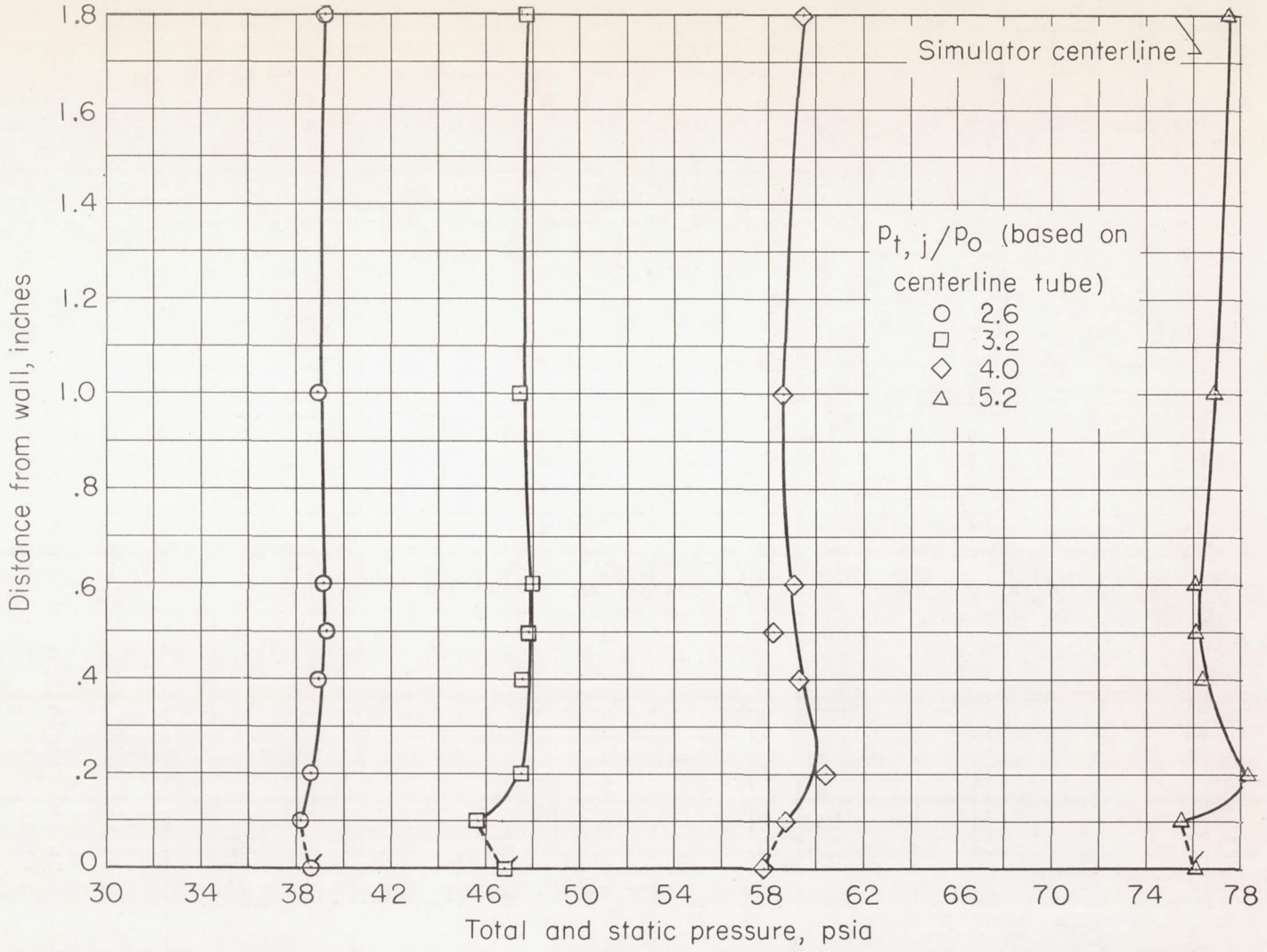


Figure 11.- Total-pressure variation at x = 16.7 from simulator wall to center line at several jet total-pressure ratios. Flagged symbols are wall static pressures.

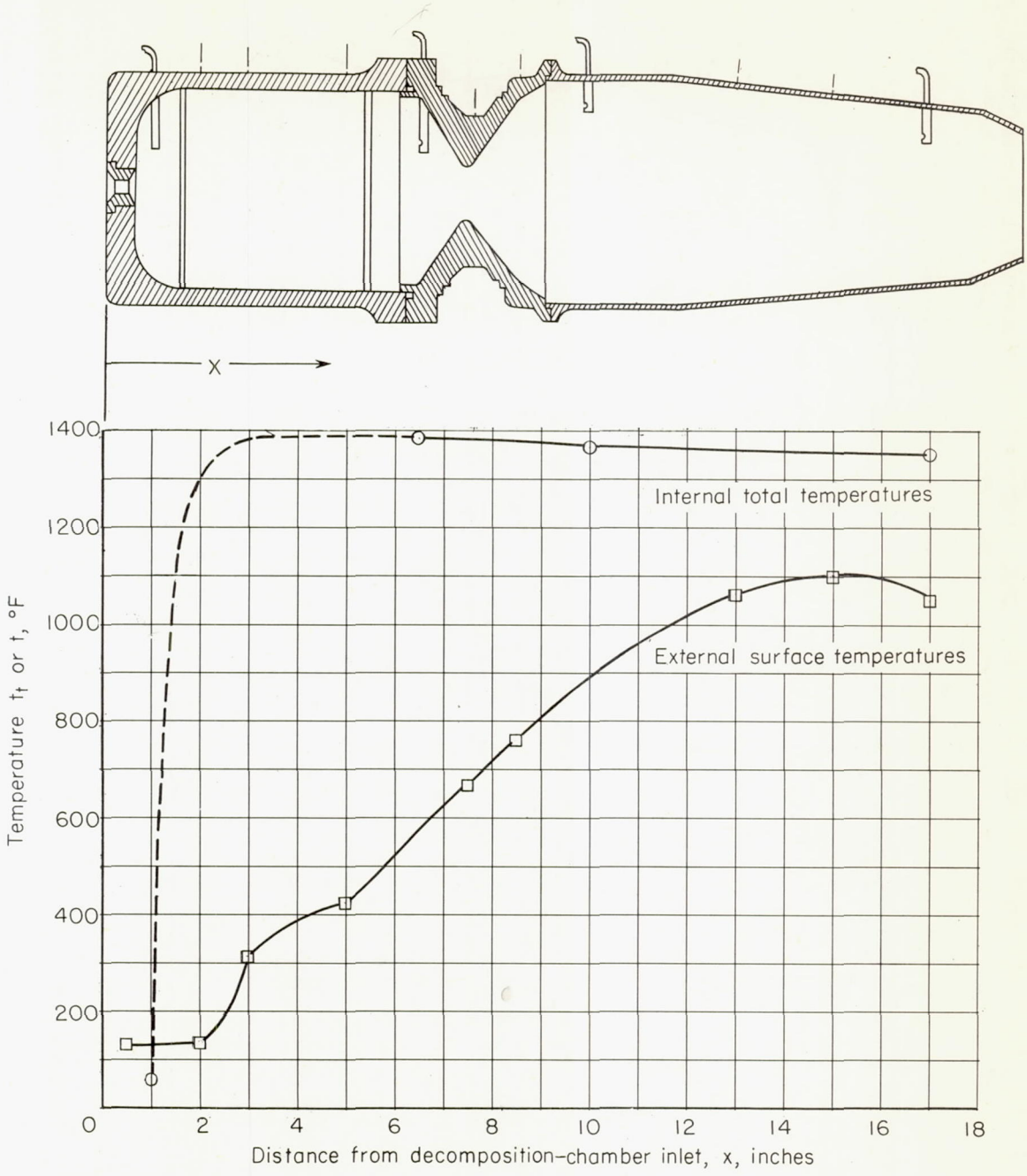


Figure 12.- Typical variation of temperature along jet simulator system. Primary system only. $t_0 = 62^\circ$ F; $p_{t,j}/p_0 = 2.8$.

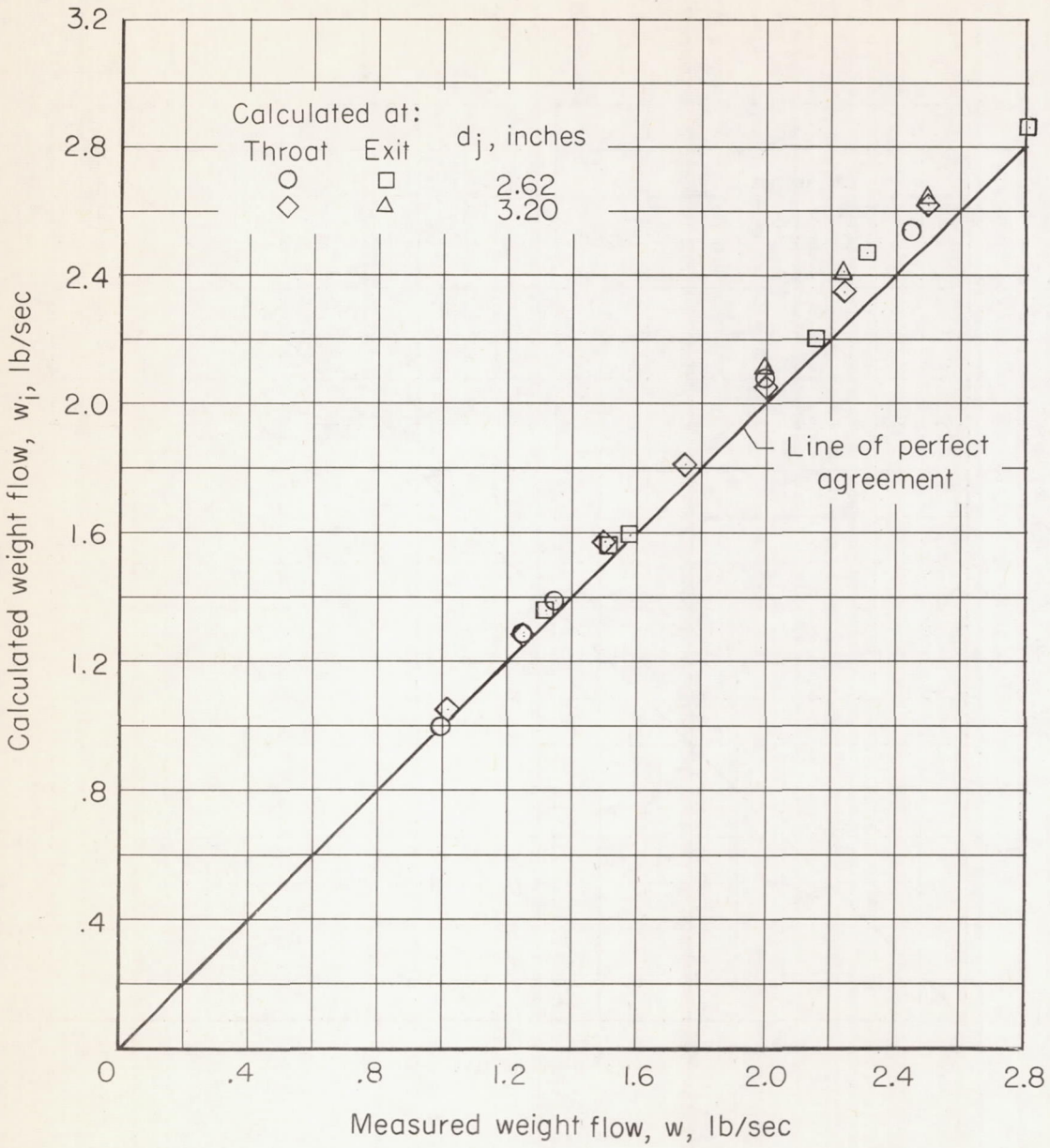


Figure 13.- Comparison of flow rates calculated from gas measurements with liquid-flowmeter measurements. Convergent nozzles.

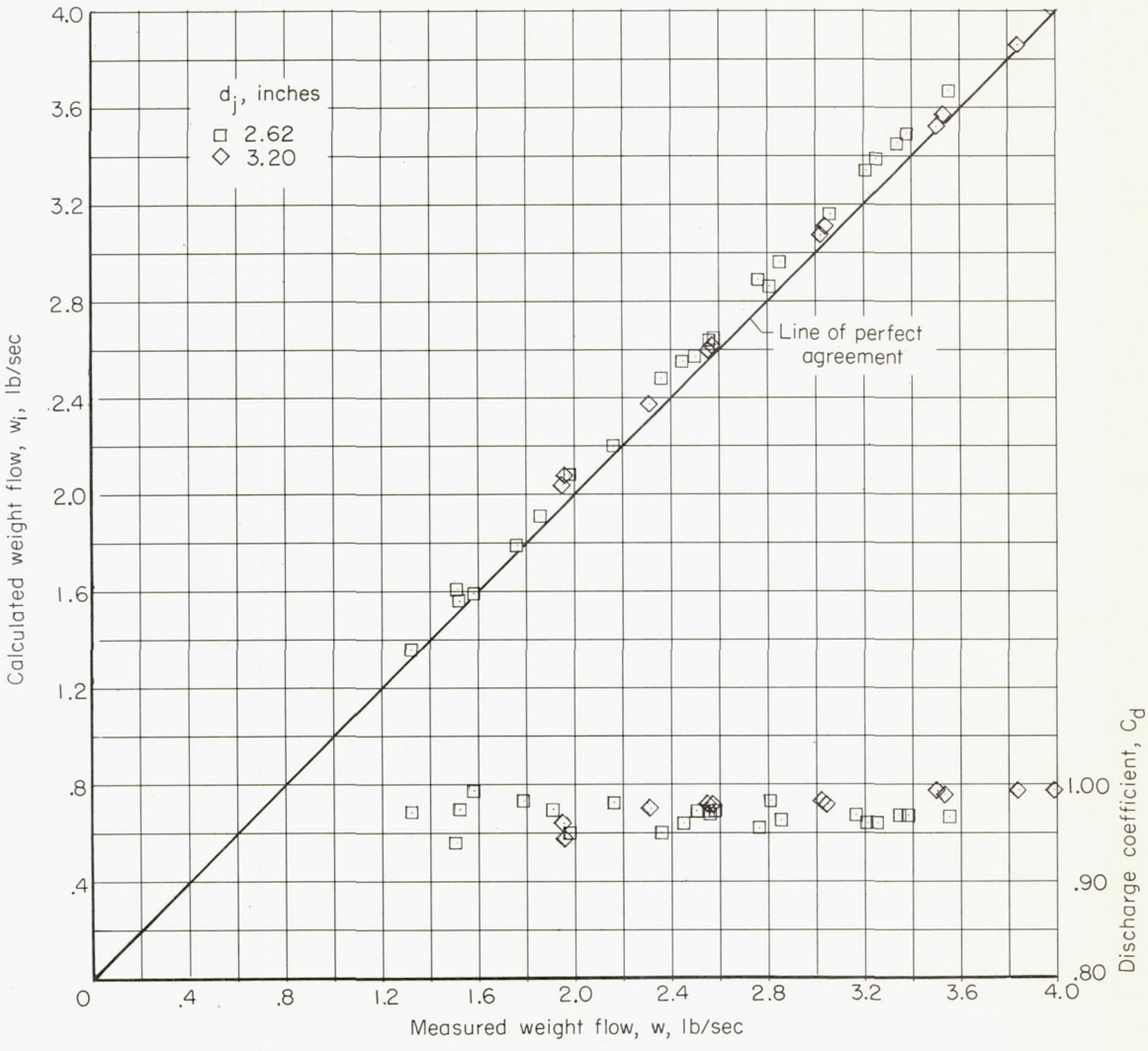


Figure 14.- Discharge coefficient for sonic nozzles.

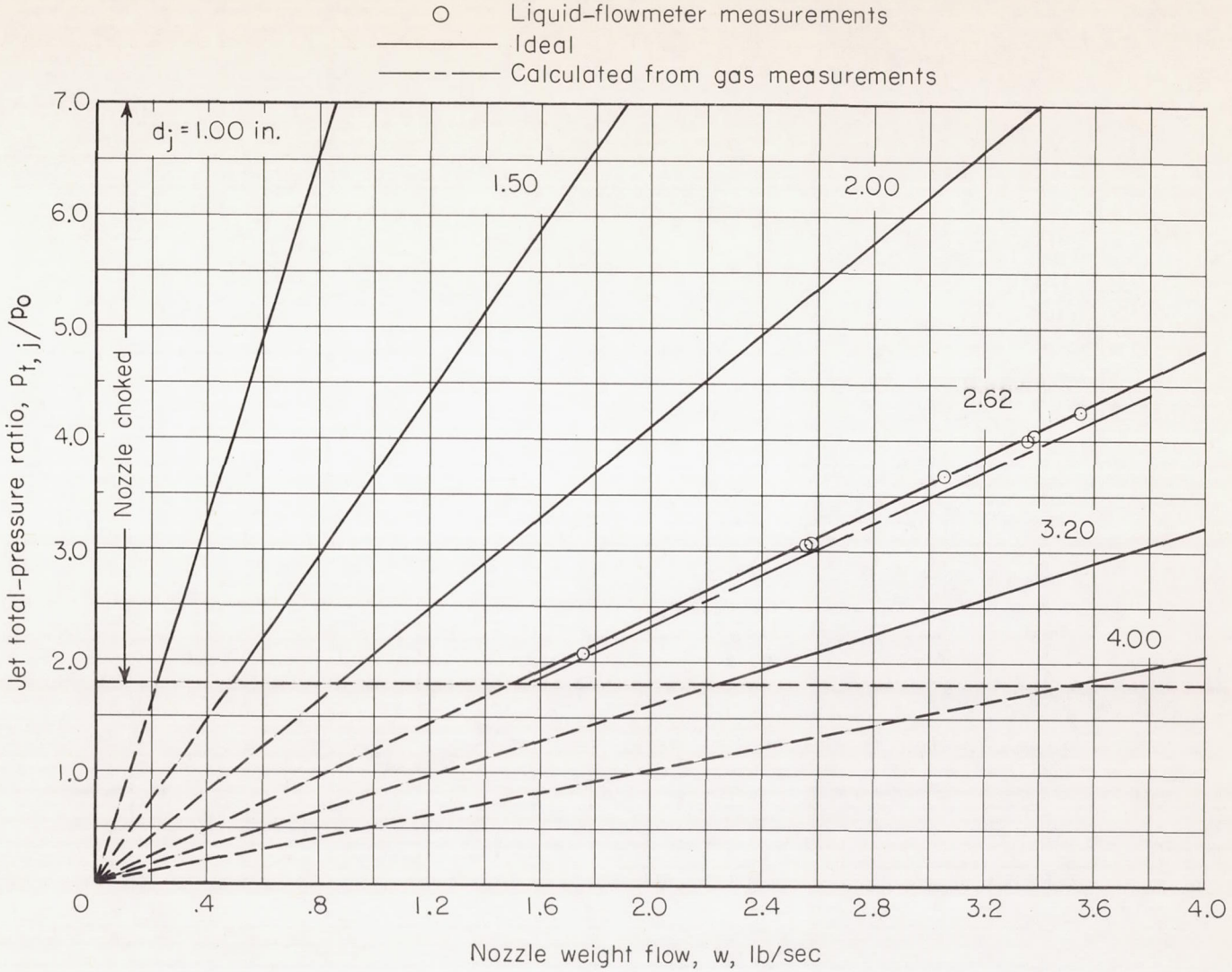


Figure 15.- Variation of jet total-pressure ratio with nozzle jet weight flow for convergent sonic nozzles with hydrogen peroxide jets. Standard NACA day.

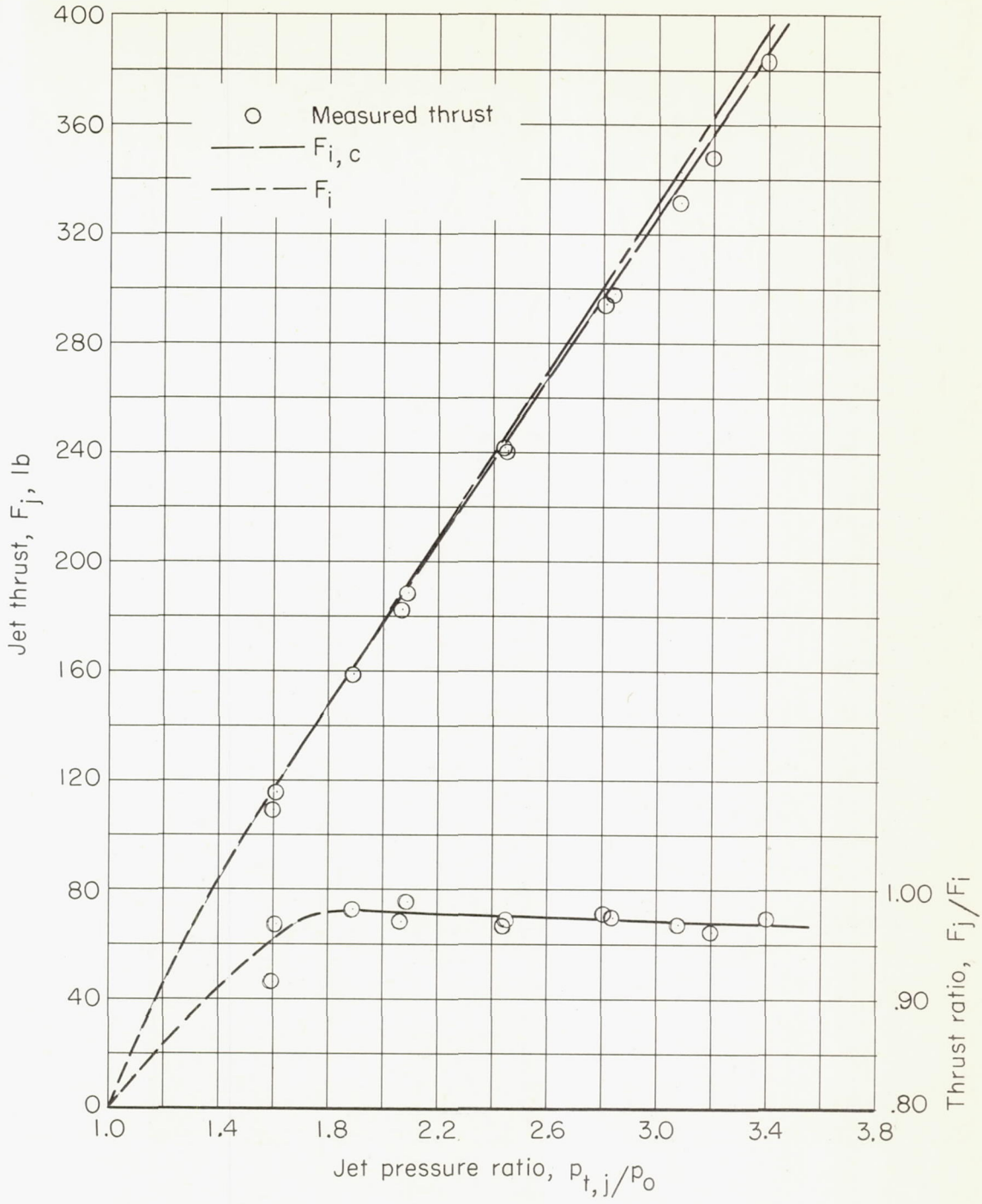


Figure 16.- Variation of jet thrust and thrust ratio with pressure ratio. Convergent nozzle; d_j = 3.20 in.

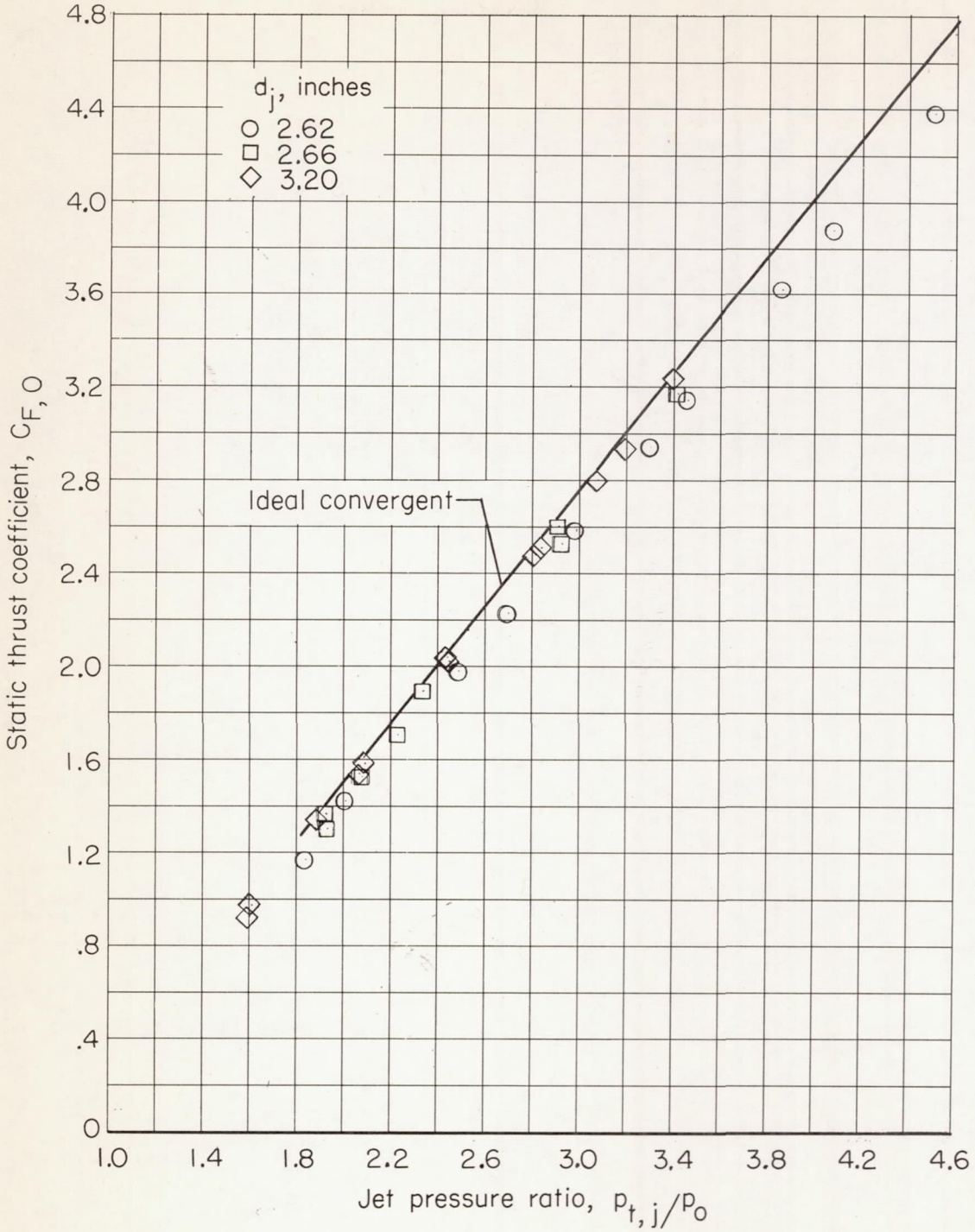


Figure 17.- Variation of static thrust coefficient with jet pressure ratio for several convergent nozzles.